forests

MDPI

Article

Carbon Sink Performance Evaluation and Socioeconomic Effect of Urban Aggregated Green Infrastructure Based on Sentinel-2A Satellite

Shuoqi Cheng [1], Xiancheng Huang [2], Yu Chen [1,*], Hangna Dong [1] and Jing Li [3]

[1] Department of Landscape Architecture, Nanjing Agricultural University, Nanjing 210095, China
[2] Morrissey College of Arts and Sciences, Boston College, 140 Commonwealth Ave., Chestnut Hill, Boston, MA 02467, USA
[3] Department of Chemical & Materials Engineering, University of Auckland, 0926 Auckland, New Zealand
* Correspondence: chenyu@njau.edu.cn

Abstract: Aggregated green infrastructure is the only element that has a relatively concentrated and well-functioning carbon sink in the city. It plays an important role in achieving carbon neutrality in urban areas with dense functions and scarce carbon sink resources. However, in contrast to other regions, aggregated green infrastructure carbon sink performance is more influenced by socioeconomic activities in urban centres. There is a lack of research on the impact between carbon sink performance and socioeconomic activities at the urban scale. In this study, we evaluated the carbon sink performance (i.e., carbon sink and location entropy) of aggregated green infrastructure and its interaction with socioeconomic activities at the urban scale based on Sentinel-2A satellite. The results showed that: (1) Aggregate green infrastructures with high carbon sink performance have significant aggregation characteristics in urban areas. (2) Aggregated green infrastructure with poor carbon sink performance tended to be surrounded by dense socioeconomic activities. Our study provides a new approach to the assessment of carbon sink performance of aggregated green infrastructure at the urban scale. More importantly, we make a new attempt to assess the association between carbon sink performance and socioeconomic activities of urban aggregated green infrastructure. These results point to a new direction for the realization of carbon neutrality in cities.

Keywords: aggregated green infrastructure; multi-source data; climate change; carbon sink performance

Citation: Cheng, S.; Huang, X.; Chen, Y.; Dong, H.; Li, J. Carbon Sink Performance Evaluation and Socioeconomic Effect of Urban Aggregated Green Infrastructure Based on Sentinel-2A Satellite. *Forests* **2022**, *13*, 1661. https://doi.org/10.3390/f13101661

Academic Editors: Bo Hong, Dayi Lai, Zhi Gao, Yongxin Xie and Kuixing Liu

Received: 7 September 2022
Accepted: 8 October 2022
Published: 10 October 2022

Publisher's Note: MDPI stays neutral with regard to jurisdictional claims in published maps and institutional affiliations.

1. Introduction

In the context of increasing global warming, energy and carbon emissions are increasingly influencing and constraining urban development. With the concept of "carbon neutrality", energy conservation and emission reduction have become the core of sustainable urban development [1]. In addition to reducing fixed energy use and transportation carbon emissions, increasing urban carbon sinks is also an important means to achieve "carbon neutrality" [2,3]. Previous studies on carbon sinks have mainly focused on forests, grasslands, wetlands, oceans and soils [4–7]. The carbon sink function of urban ecosystems has been neglected. Green infrastructure is a scarce resource for urban ecosystems. Some studies have shown that it plays an important role in increasing carbon sinks and absorbing carbon emissions [8,9].

The concept of green infrastructure was first introduced in the United States in 1999, and it is defined as the National Natural Life Support System. In terms of landscape pattern, it is divided into aggregated green infrastructure and distributed green infrastructure [10]. In urban area, aggregated green infrastructure is generally park with abundant vegetation resources and carbon sink capacity. Distributed Green Infrastructure is small and scattered throughout the man-made landscape as temporary habitats or "stepping stones" [11]. Forman states that the focus of the approach to landscape pattern optimization is the overall

optimization of the landscape pattern [12]. Therefore, the combination of aggregation and distribution is considered irreplaceable for the landscape pattern in terms of overall optimization. In addition, size is closely related to the carbon sequestration capacity of green infrastructure, with larger green spaces on average performing better than smaller ones [13]. According to a study, the UK government considers 2 hectares as the minimum acceptable size of green space in urban area [14]. Therefore, we use 2 ha as the threshold to define aggregated green infrastructure and distributed green base. This classification helps to extract green infrastructure with significant carbon sink capacity and facilitates the study in urban areas.

Aggregated green infrastructure is an urban complex ecosystem with a significant ecological service function. It can fix carbon and release oxygen [15], effectively alleviate the heat island effect [16], and reduce urban energy consumption [17]. It is an important carrier for carbon peaking and carbon neutrality [18,19]. In this study, the carbon sink performance of aggregated green infrastructure mainly refers to the efficiency of their carbon sinks within their service scope. At present, the aggregated green infrastructure carbon sink performance study includes the following three main aspects: (1) evaluating the carbon sink capacity of aggregated green infrastructure systems at the macro scale based on different types of vegetation through the City green model [20,21]; (2) calculating the carbon sink benefits of different tree species using biomass method, regression equation calculation method, photosynthetic rate method at the microscopic scale [22–24]; (3) assessing of aggregated green infrastructure carbon sink performance was mainly based on the carbon sink efficacy of plants at the mesoscopic scale [25,26]. The conclusions are often subject to a large margin of error, and the results are significantly less compared to the first two aspects. Many previous research data are limited to the carbon storage and sequestration benefits of single plant species and individual vegetation type. They have made it difficult to directly assess the carbon sequestration performance of aggregated green infrastructure in terms of the overall model. Furthermore, it is well known that unlike natural green spaces such as forests, human socioeconomic activities have a greater impact on the carbon sink capacity of aggregated green infrastructure in cities [27,28]. Due to data limitations, previous studies were mostly limited to the effects of population, GDP, and road density on the overall urban green infrastructure carbon sink capacity [29–31]. Currently, few studies have explored the coupling between the carbon sink performance of aggregated green infrastructure and the socioeconomic activities of inner cities. In general, there is a lack of results on the ability to comprehensively assess the total carbon sink of aggregated green infrastructure at the city scale and analyse its association with socioeconomic activities.

Sentinel missions are joint initiative of the European Commission and European Space Agency and its information is available for free. The latest land cover information, including urban aggregated green infrastructure is a high-resolution optical satellite Sentinel-2A observation mission [32]. Sentinel-2A satellite was launched in 2015 and has a spatial resolution of up to 10 m $\times$ 10 m [32,33]. It has a higher spatial resolution than Landsat 8 satellite data, which is also available free of charge. The cost is lower than that of commercial satellites. It has been applied to fine scale remote sensing studies in multiple fields such as environment and ecology [34–36]. The spatial structure of urban aggregated green infrastructure is complex including vegetation, water bodies and roads. It is on a much finer scale than the others. Therefore, we try to use Sentinel-2A satellite to discern aggregated green infrastructures within cities in order to calculate their carbon sink performance. Furthermore, POI data performs well in terms of timeliness and allows for a more flexible and specific response to inner city functions. It has been used in studies to explore socioeconomic activity studies within and outside the city [37–39]. Therefore, this study aims to explore the association between socioeconomic effects and the carbon sink performance of aggregated green infrastructure at the intra-city level based on Sentinel-2A and POI data. The overall goals are: (1) to calculate aggregated green infrastructure carbon sequestration amount by Sentinel-2A satellite information, and use location entropy to evaluate their carbon sink performance; (2) to evaluate the spatial distribution characteristics of

aggregated green infrastructure carbon sink performance in central urban area of Nanjing on spatial autocorrelation; (3) to assess the relationship between the spatial distribution of aggregated green infrastructure carbon sink performance and socioeconomic activities on the POI (Point of Interest).

2. Materials and Methods

2.1. Research Area

Nanjing City (31°14″−32°37″ N, 118°22″−119°14″ E) is located in East China. It is a typical subtropical monsoon climate with hot summers and abundant rainfall, cold and dry winters, and cool and dry springs and autumns. The vegetation types are mainly deciduous broad-leaved forests that contain evergreen broad-leaved trees and planted coniferous forests. The study area is the central urban area delineated in the Draft Nanjing Urban Master Plan (2018–2035). The total area is about 818 square kilometres, accounting for about 12.42% of the total area of Nanjing. The delimitation of the research area is mainly based on the following three considerations: (1) the city centre area has a dense built environment and population distribution, which is suitable for studying the interaction between the daily life behaviour of individual residents and the aggregated green infrastructure; (2) the commodity housing prices in Nanjing have generally maintained an upward or stable trend and never experienced a significant decline since the 21st century; (3) the POI of the average price, population, transportation, businesses, entertainment, and public facilities in the residential area of the city centre is easily accessible.

2.2. Data Source

2.2.1. Aggregated Green Infrastructure Data

The study adopted the vectorized extraction operation of the non-offset Google Earth high-definition satellite imagery of Nanjing in 2021 to demonstrate aggregated green infrastructure boundary. Then, a total of 90 aggregated green infrastructures within the central urban area of Nanjing were selected accordingly, under the guidance of the Draft of Nanjing Urban Master Plan (2018–2035) the correction of on-the-spot investigation (Figure 1).

The remote sensing data came from the data of ESA's Sentinel-2A satellite. The imaging time is July 30, 2021. It has a 0.0174% of cloud with a resolution of 10 m. The SNAP software was used for pre-processing: cutting according to the scope of the park and using Envi-met to perform radiometric calibration and atmospheric correction on the remote sensing images. The study interpreted and divided aggregated green infrastructure landscape elements in the central urban area of Nanjing into three types of carbon sinks: woodland, grassland, and water.

2.2.2. Socioeconomic Activities Data

To effectively reflect the activity intensity of the users, the study screened various network data and selected socioeconomic activities data that are closely related to aggregated green infrastructure. The influencing factors of recreational activities in aggregated green infrastructures can be roughly summarized as accessibility, population distribution, and socioeconomic status of the population [5,10]. Therefore, the study selected six factors including transportation convenience, the richness of cultural and recreational facilities, employment opportunities, public service convenience, the number of residents, and income as the main influencing factors for human activities. The source of the data came from six origins, i.e., POI for transportation facilities; POI for dining and shopping; POI for companies; POI for public facilities; the number of residential households; the average house. The POIs were captured by Python tool and collected in July 2020 and May 2021. According to the 2020 Nanjing Statistical Yearbook, the average household population in Nanjing urban area is 2.77 people, which can be used to estimate the population of each community (Table 1).

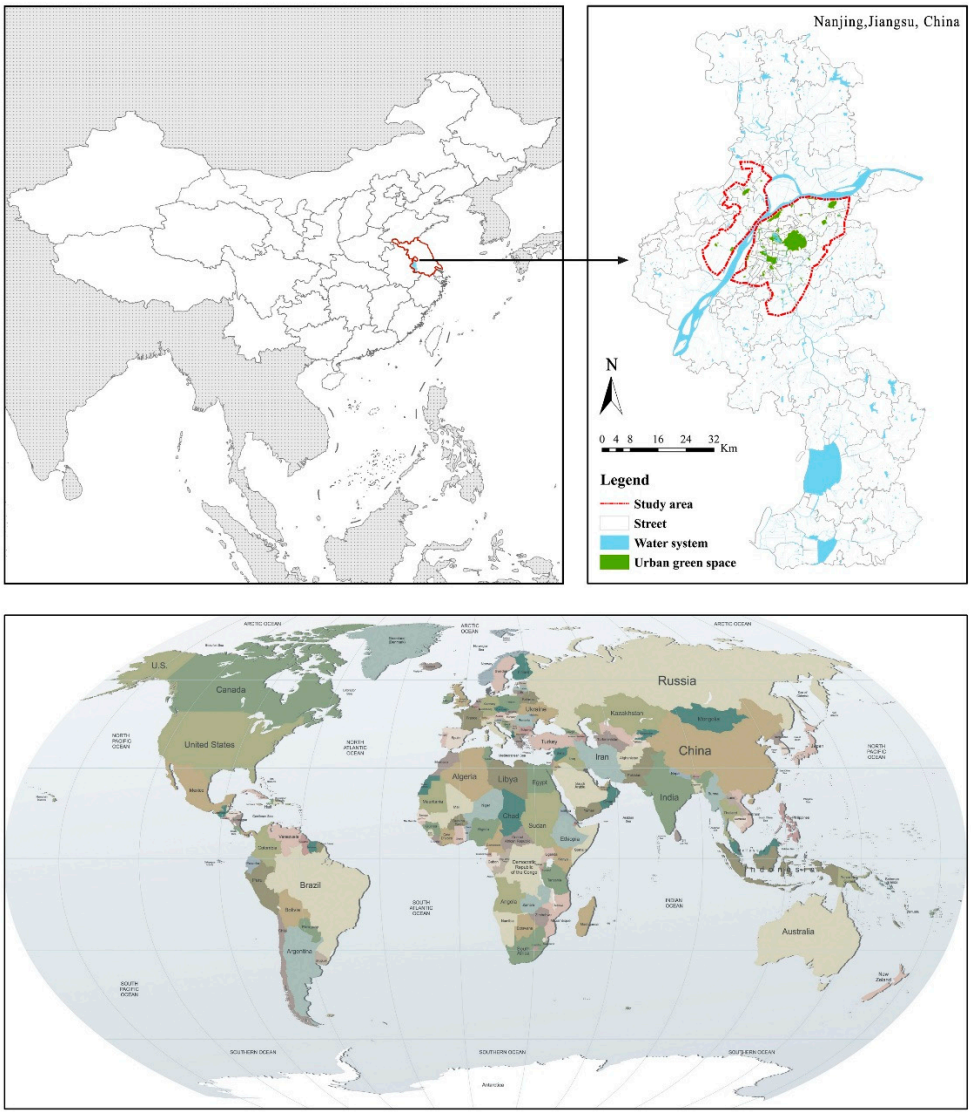

Figure 1. Location of central Nanjing, China.

Table 1. Socioeconomic activities data sources.

	Indicators	Data
Socioeconomic status	The income of residents	Average house price
Population Distribution	The number of residents	Number of households × Average Population per household
Accessibility	Public service convenience	Number of public facility POIs
	Employment opportunities	Number of company POIs
	The richness of cultural and Recreational facilities	Number of dining and shopping POIs
	Transportation convenience	Number of transport facilities POIs

2.3. Method

Previous studies have shown that many cities have implemented the low carbon city evaluation index system [40,41]. Among the indexes, the green environment construction and carbon sink capacity were the main evaluation indicators [42]. Therefore, based on the obtained data and the previous-built carbon sink city evaluation systems, the study regarded aggregated green infrastructure environment construction and carbon sink capacity as the influencing factors of its carbon sink performance in the central urban area of Nanjing. We selected aggregated green infrastructure area and density as the

influencing factors of aggregated green infrastructure construction. In the meantime, the carbon sequestration amount of aggregated green infrastructure and location entropy were selected as the influencing factors of the carbon sink performance of aggregated green infrastructure. The analysis was performed in combination with socioeconomic activities data, and a more in-depth discussion on urban carbon sink performance was conducted based on urban development laws. The detailed experimental steps are shown in Figure 2.

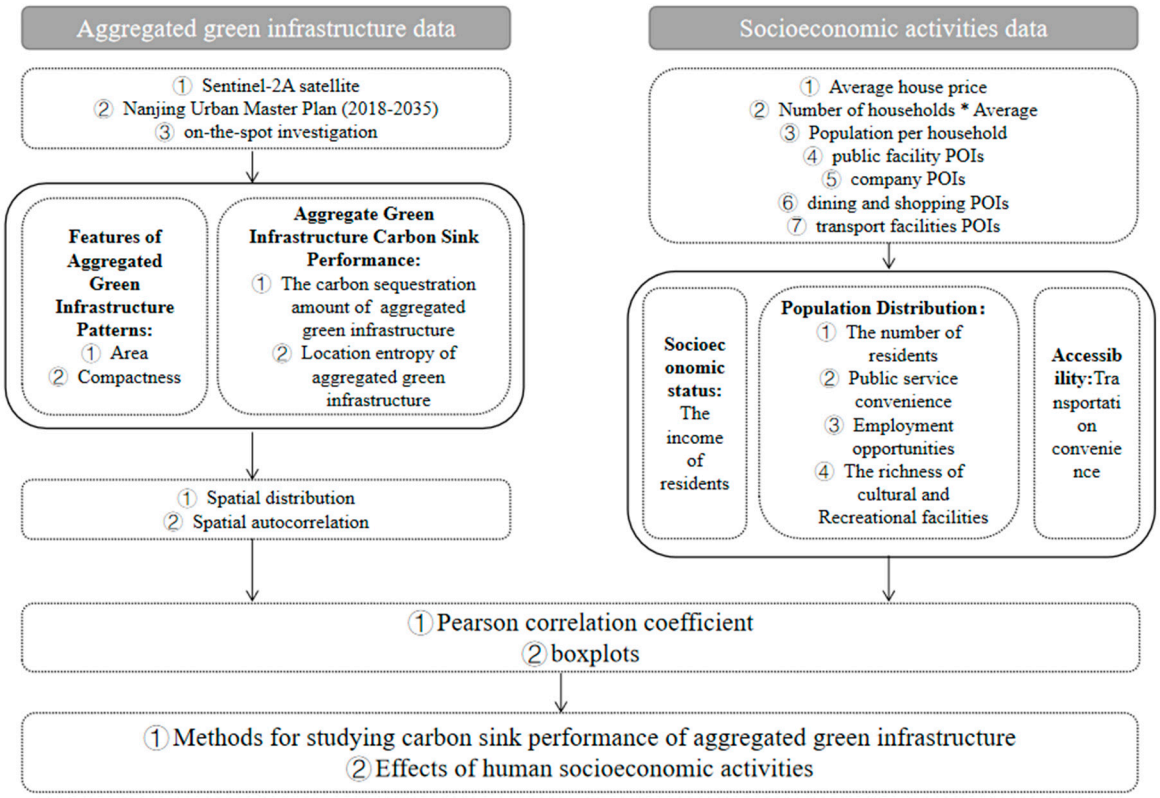

Figure 2. Experimental method step diagram.

2.3.1. The Carbon Sequestration Amount of Aggregated Green Infrastructure

The study divided the aggregated green infrastructure carbon sink into three types: woodland, grassland, and water (Table 2). Based on the three types, the calculation model of carbon sequestration amount of aggregated green infrastructure in the central urban area of Nanjing is constructed:

$$C_s = \sum C_{F,i} * A_i \quad (1)$$

C_s is the net carbon sequestration of the area (t/a); $C_{F,i}$ is the annual net carbon sequestration per unit area of the *i*-th type of carbon sink (t/(ha·a)), and Ai is the total area of the *i*-th type of carbon sink (ha).

Table 2. Carbon sink factor.

Parameter Category	Value	Source
forest land carbon sequestration (t/(ha·a))	9.0300	[43]
Grassland carbon sequestration (t/(ha·a))	7.7100	[44,45]
water area carbon sequestration (t/(ha·a))	2.0900	[46]

2.3.2. Location Entropy of Aggregated Green Infrastructure

The study used location entropy to analyse the spatial distribution of aggregated green infrastructure carbon sink performance in each city [47]. Location entropy is also called specialization rate. It was first proposed by Hagget and applied to location analysis. Location entropy is efficient in measuring the spatial distribution of certain regional elements. It has been widely used in the evaluation of industrial agglomeration. The calculation formula is:

$$L_{Q_i} = (T_i/P_i)/(T/P) \quad (2)$$

In the formula, L_{Qi} represents the location entropy of the aggregated green infrastructure carbon sink of the city i; T_i is the carbon sink level of the aggregated green infrastructure in the city i, i.e., carbon sequestration amount; P_i represents the area of the aggregated green infrastructure in the city i; T is the total carbon sequestration amount of aggregated green infrastructure within the study area; P represents the total area of aggregated green infrastructure within the study area. Location entropy represents the ratio of the carbon sink level of a city's aggregated green infrastructure to the average carbon sink level of all aggregated green infrastructures within the study area. If the location entropy is greater than 1, it will indicate that the city's aggregated green infrastructure carbon sink level is higher than the average level of the study area, and vice versa.

2.3.3. Compactness of Aggregated Green Infrastructure

It has been confirmed that carbon sequestration amount is related to the spatial layout of carbon sink elements. In order to explore the relationship between the carbon sink level and the spatial layout of aggregated green infrastructure, the study adopted the Richardson index to quantify the compactness of aggregated green infrastructure within the research area [14].

$$C = 2\sqrt{\pi * A}/P \quad (3)$$

C is the compactness; A is the actual aggregated green infrastructure area; P is the circumcircle circumference. The larger the value of C, the closer the shape of the aggregated green infrastructure is to a circle, the more likely the shape presents as block-shaped. The smaller the value of C is, the more the shape of the aggregated green infrastructure deviates from the circle and is in the shape of a band.

2.3.4. Spatial Autocorrelation

Spatial autocorrelation can analyse the law of spatial distribution. The study focused on the correlation between a certain attribute value of a unit in space and that of the surrounding units, and then analysed the statistical distribution law of spatial units and the correlations of different spatial data. It can be divided into global space autocorrelation and local space autocorrelation. Global spatial autocorrelation is used to describe the overall distribution of things and analyse the spatial agglomeration of things, while local spatial autocorrelation is to analyse the correlation between a certain element in space and its adjacent elements [47,48].

The value range of the global Moran's I is $[-1, 1]$. When the I has a positive value, it means that the space is positively correlated, and the spatial units tend to aggregate; when taking a negative value, it means that the space is negatively correlated, and the spatial units tend to be spatially discrete; while 0 means that the spatial units are randomly distributed. The significance test is usually performed with the Z value. When $|Z\ score| > 1.96$ ($p = 0.05$), it indicates that there is significant spatial autocorrelation. If I_i (local autocorrelation index of the i-th street) > 0 in the local spatial autocorrelation index (LISA) agglomeration graph, it indicates that the equivalent values of adjacent streets are similar ("low–low" or "high–high"); if $I_i < 0$, it indicates that the equivalence values of adjacent streets are dissimilar ("low–high" or "high–low").

3. Results

3.1. Spatial Distribution Analysis of Aggregated Green Infrastructure Carbon Sink Performance

3.1.1. Aggregated Green Infrastructure Carbon Sequestration

There are three types of carbon sinks extracted based on remote sensing information: forest land, grassland, and water area. The carbon sequestration model and related parameters were adopted to calculate the total annual CO_2 sequestration in the aggregated green infrastructure in the central urban area of Nanjing, which reached 34,439.78 t/a (Table 3). After calculating the carbon sequestration amount of 90 aggregated green infrastructures in the central urban area of Nanjing respectively, the study found a significantly large standard deviation of the central urban area of Nanjing, which was at 2354.3169 t/a. It is shown that the carbon sequestration capacity of aggregated green infrastructures in Nanjing had a relatively large variation, with a middle range of 4.7915−96.4523 t/a (Table 4).

Table 3. Carbon sequestration in each carbon sink of urban green space in central Nanjing.

Carbon Sink	Area (ha)	Carbon Sink Volume (t/a)
Forest land	3386.10	30,576.48
Grassland	349.58	2695.26
Water area	558.87	1168.04
Total	4987.13	34,439.78

Table 4. Statistical characteristics of in each carbon sink of urban green space in central Nanjing.

Statistical Characteristics	Carbon Sink Volume (t/a)
Sample size	90
Min	0.1922
Max	22,157.1381
Mean	375.6586
Standard Deviation	2354.3169
Upper quartile	4.7915
Median	27.2026
Lower quartile	96.4523
Quartile distance	69.2496

3.1.2. Spatial Distribution of Aggregated Green Infrastructure Carbon Sink Performance

The study paid close attention to the needs of residents' well-being and sets a threshold of 1200 m, a 15-min walking distance, to delineate the service range along the boundary of aggregated green infrastructure [14]. It is set to characterize the range of residents' daily activities and life trajectories. Under this scenario, the allocation of the aggregated green infrastructure resources that residents can enjoy in their daily lives is rationally monitored accordingly. The study superimposed the above-mentioned six types of data and the aggregated green infrastructure service range that satisfies the above two factors for further analysis. In the meantime, the factors of carbon sequestration amount and location entropy are selected to characterize the carbon sink performance of aggregated green infrastructure. The carbon sequestration amount of aggregated green infrastructure was evenly divided into three parts according to the numerical value, while location entropy was divided into two parts the average amount "1" as the boundary. The service area was measured according to the street unit and the natural interval method. The natural breakpoint method was adopted to divide the service area of each street into three categories: high, medium, and low.

The effective carbon sequestration area of the aggregated green infrastructure with an area larger than 100 ha is the highest, which should be attributed to the excellent ecological environment. The highest annual carbon sequestration is 22,157.1381 t/a. These aggregated green infrastructures are mainly located in the central and northeastern areas of the city. Due to the natural landscape pattern and the age of urban development, only a few clustered green infrastructures are located in the northwestern part of the city. Their carbon

sink performance tends to be poor. Most of the aggregated green infrastructures with low carbon sequestration amount were located in the high-density central old urban area. The carbon sequestration amount of them was less than 1 t/a. They were generally small in these areas, which was related to their lack of better ecological benefits. In addition, the central urban area was resource-intensive with frequent Socioeconomic activities, which also caused more challenges to build medium and large aggregated green infrastructures with strong carbon sequestration capabilities. In general, the carbon sequestration capacity of aggregated green infrastructures in the central urban area of Nanjing varies, and the northwestern part of the city lacked aggregated green infrastructures with high carbon sequestration capability.

Results of the location entropy of aggregated green infrastructure showed 72 aggregated green infrastructures have a location entropy of less than 1, densely distributed in the central old urban area. The green spaces of northwestern part of the city area all had a location entropy of less than 1, exhibiting a relatively bad performance of aggregated green infrastructure carbon sinks. There were a total of 18 aggregated green infrastructures with a location entropy greater than 1, which were concentrated in the central old city and northwestern part of the city. Overall, the carbon sink performance of aggregated green infrastructures in the central urban area of Nanjing varies, and northeast of the city lacked aggregated green infrastructure with better carbon sink performance (Figure 3).

3.1.3. Spatial Autocorrelation of Aggregated Green Infrastructure Carbon Sink Performance

From the perspective of carbon sequestration amount, spatial autocorrelation analysis showed that the first group of carbon sequestration exhibited the largest Moran's I index and the largest Z value, while the third group showed the smallest Moran's I index and the smallest Z value (Table 5). It indicated that the aggregated green infrastructures with small carbon sequestration amounts had a relatively high degree of aggregation. In addition, the *p* values of carbon sequestration in the three groups were all less than 0.01, indicating that the carbon sequestration in the three groups had extremely significant space autocorrelation. From the perspective of location entropy, the largest Moran's I index of location entropy appears in the first group, and it also showed the largest Z value. However, the second group exhibited the smallest Moran's I index of location entropy and the smallest Z value. It indicated that aggregated green infrastructures that have less location entropy will appear relatively significant space aggregation. In the meantime, the *p*-values of the two groups were both less than 0.01, indicating that the two groups had extremely significant space autocorrelation. Overall, the lower the carbon sequestration amount in aggregated green infrastructure, the more significant the spatial correlation, and vice versa.

Table 5. Moran's I index of carbon sink performance of aggregated green infrastructure.

Indicator	Group	Moran's I	Z Value	*p* Value
Carbon sink	Group1	0.4192	13.9772	0.0000
	Group2	0.1826	5.9574	0.0000
	Group3	0.1522	5.4640	0.0000
Location entropy	Group1	0.4369	14.1768	0.0000
	Group2	0.2076	6.7441	0.0000

From the perspective of carbon sequestration amount, it can also be seen the first group is dominated by low–low clusters: a total of 24 streets of this type are distributed in the northern urban area. In addition, there are 11 streets in the high–high cluster type and 10 streets in the low–high cluster type, mainly distributed in the central old city. The second group is dominated by high–high clusters with a total of 15 streets, mainly distributed in the central old city. In addition, there are 14 low–low clusters, 2 high–low clusters, and 7 low–high clusters, distributed at the edge of the central urban area. The third group is dominated by low–low clusters: a total of 18 are distributed in the northwestern and southwestern parts of the city. It has a total of 4 low–high clusters, and 10 high–high clusters, distributed

in the northwest of the central urban area. From the perspective of location entropy, the first group demonstrated both 17 high–high and low–low clusters. The high–high clusters were distributed in the central urban area, and the low–low clusters were distributed in the north of the central urban area. In addition, there were a total of 13 streets in the low–high cluster type, which were distributed in the central old city. The second group of high–high clusters showed a total of 14 streets, distributed in the northwest of the central city. There were 12 streets in low–low cluster type, distributed in the southwest of the central city. There were respectively 2 streets in low–high clusters and high–low clusters, distributed in the fringe area of the central urban area. In summary, the aggregated green infrastructures with lower carbon sequestration amount and location entropy were concentrated in the central old city, and those with higher indexes were concentrated in the southwest of the central city. It showed that aggregated green infrastructures with low carbon sink performance were concentrated in the central old urban areas, and those with higher performance were concentrated in the southwest of the central city with better natural resources. Combined with the global spatial autocorrelation analysis, results showed that aggregated green infrastructures with low carbon sink performance had the most significant feature of space agglomeration (Figure 4).

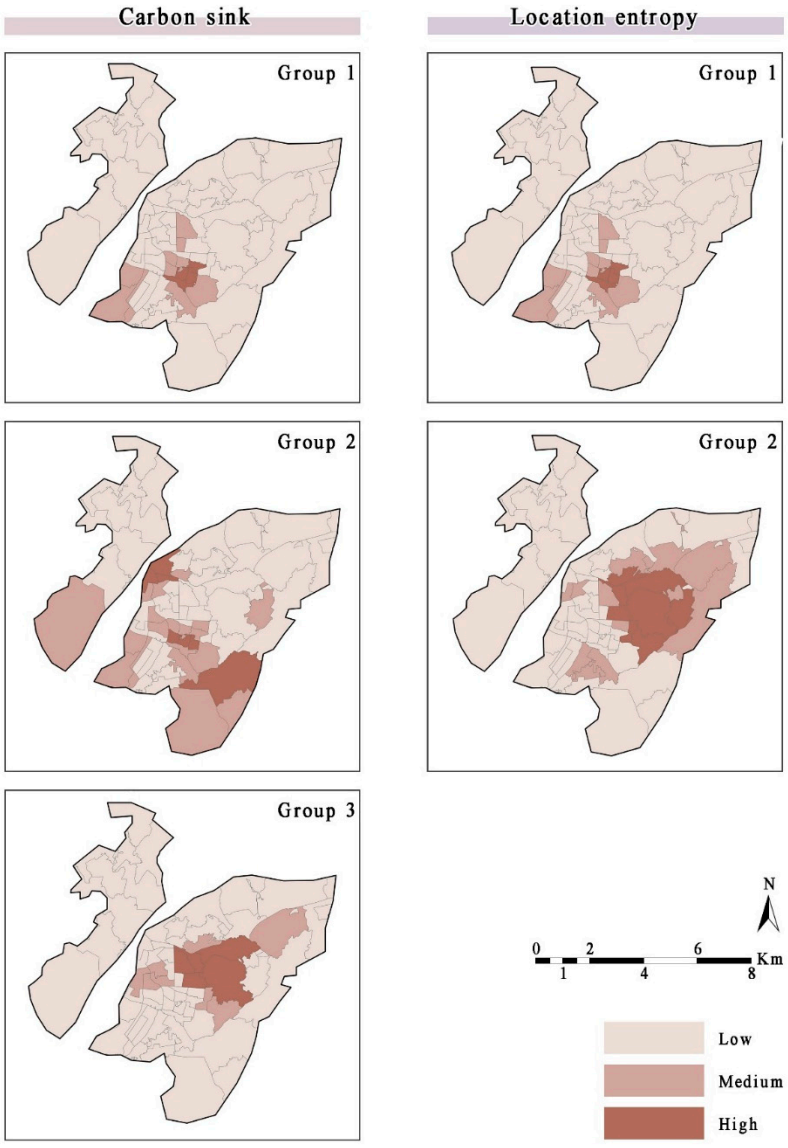

Figure 3. Spatial distribution of carbon sink performance in aggregated green infrastructure.

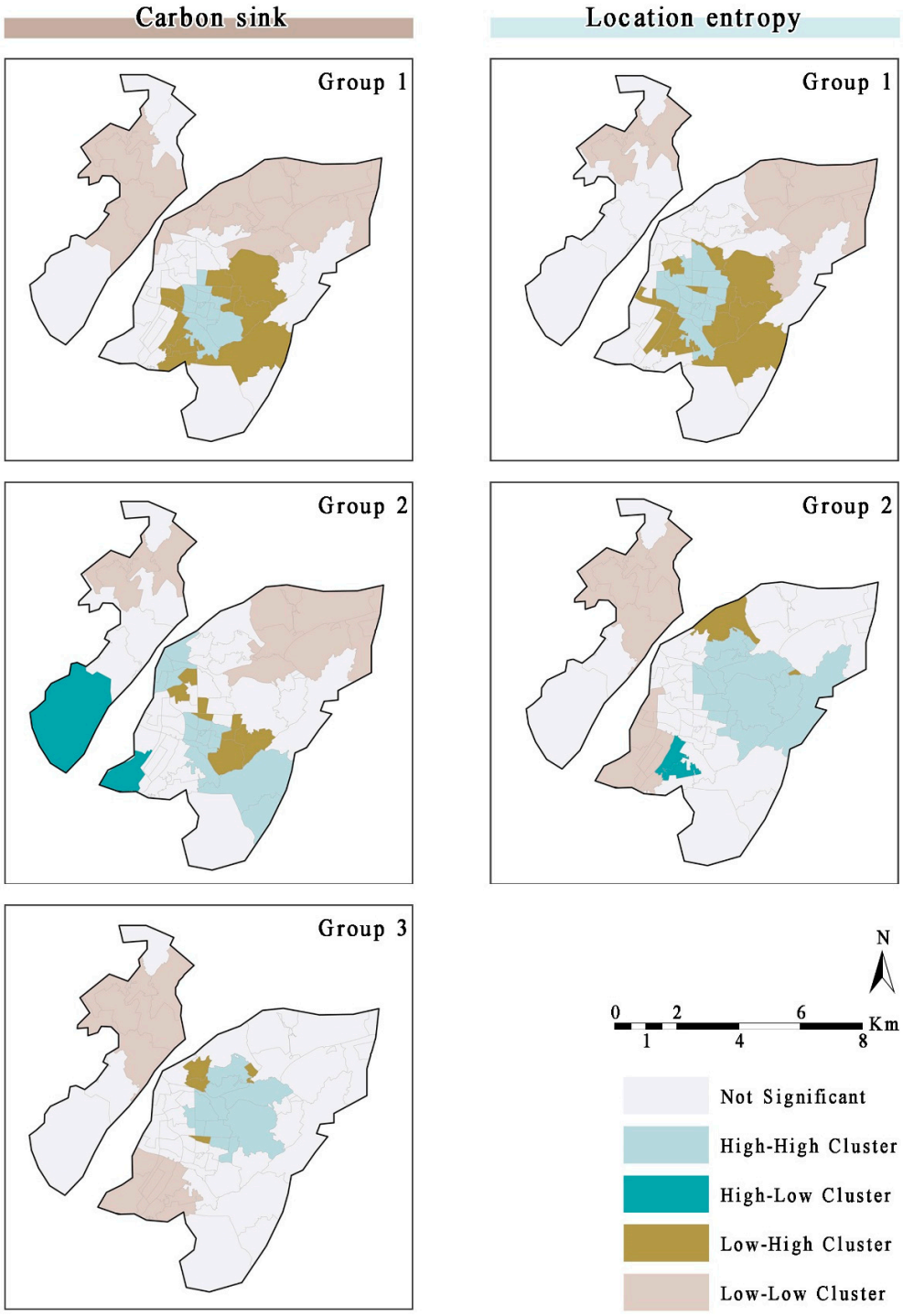

Figure 4. LISA of carbon sink performance of aggregated green infrastructure.

3.1.4. Spatial Distribution Statistical of the Socioeconomic Activities and Aggregated Green Infrastructure Carbon Sink Performance

In the paper, boxplots were adopted to analyse the correlation characteristics between factors. After comparing the correlation between aggregated green infrastructures with different carbon sequestration levels and human activities, it presented the following six types of data, i.e., the population, income, employment opportunities, and richness of cultural and recreational facilities within the area (Table 6). All exhibited good value if the carbon sequestration amount was in the range of 0.1922–7.5511 t/a. It means that aggregated green infrastructures with this range of carbon sequestration amount have

more population, higher income, and more employment opportunities. This range also indicated better transportation convenience, better public service convenience, and more cultural and entertainment facilities. After comparing the relationship between aggregated green infrastructures of different location entropy and human activities, it is found that the six types of data (i.e., the population, income, transportation convenience, public service convenience, employment opportunities, and cultural and recreational facilities richness within the area) presented good value when location entropy was in the range of 0.0387-1. It means that the aggregated green infrastructures with this range of location entropy have more population, higher population income, better transportation convenience, better public service convenience, more employment opportunities, and more cultural and recreational facilities (Figure 5).

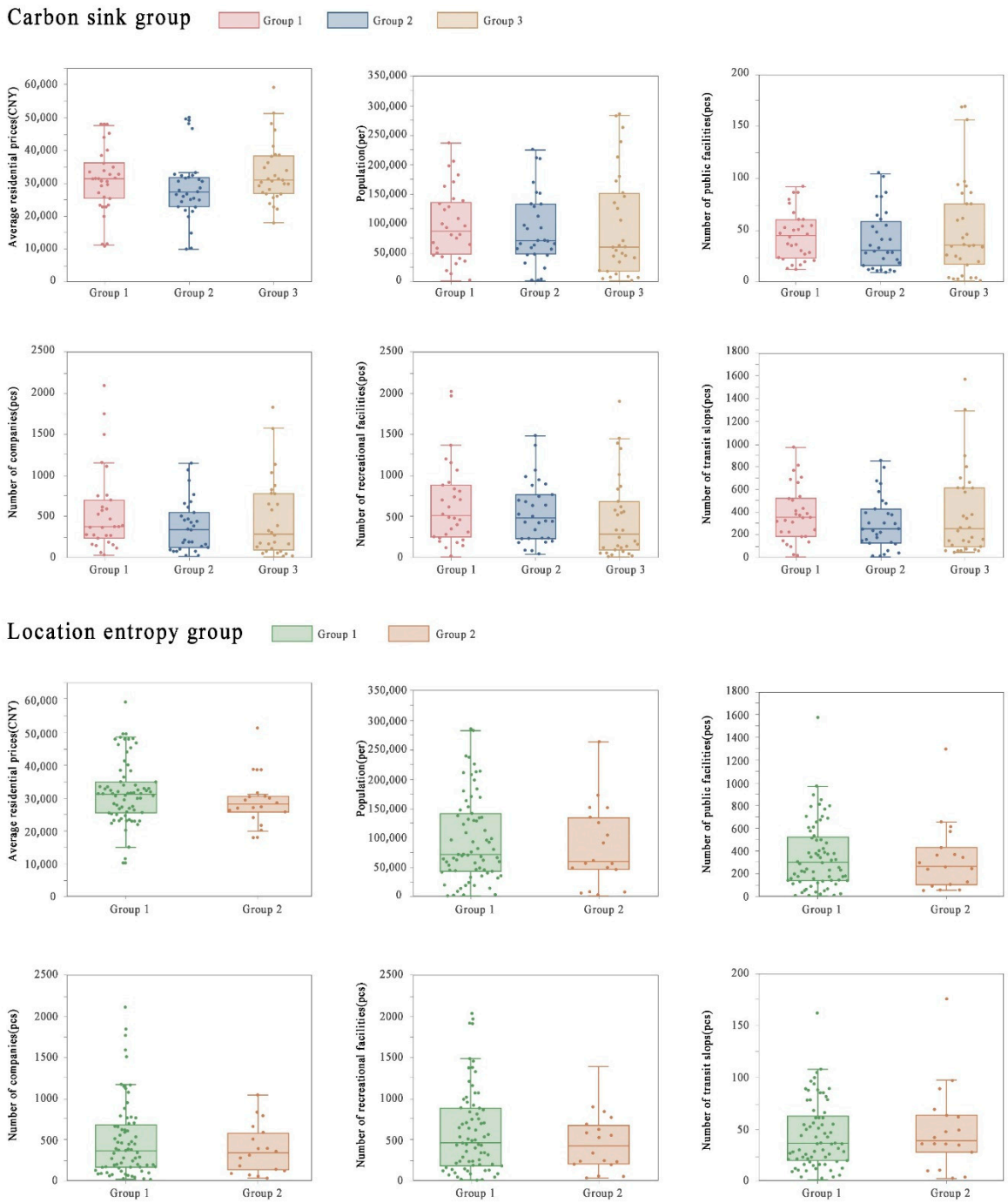

Figure 5. Box plot of Socioeconomic activities.

Table 6. Pearson correlation coefficient.

Variables	Area	Shape	Carbon Sink Volume	Location Entropy	The Income of Residents	The Number of Residents	Public Service Convenience	Employment Opportunities	The Richness of Cultural and Recreational Facilities	Transportation Convenience
Area	1	−0.03 (0.778)	0.993 ** (0)	0.206 (0.051)	−0.015 (0.885)	0.273 ** (0.009)	0.466 ** (0)	0.174 (0.102)	0.211 * (0.046)	0.397 ** (0)
Shape	−0.03 (0.778)	1	−0.036 (0.738)	0.107 (0.315)	−0.121 (0.256)	−0.309 ** (0.003)	−0.317 ** (0.002)	−0.119 (0.263)	−0.216 * (0.041)	−0.279 ** (0.008)
Carbon sink volume	0.993 ** (0)	−0.036 (0.738)	1	0.223 * (0.035)	−0.025 (0.818)	0.246 * (0.019)	0.435 ** (0)	0.143 (0.18)	0.184 (0.082)	0.355 ** (0.001)
Location entropy	0.206 (0.051)	0.107 (0.315)	0.223 * (0.035)	1	−0.143 (0.179)	−0.109 (0.304)	0.012 (0.914)	−0.163 (0.125)	−0.178 (0.094)	−0.081 (0.448)
The income of residents	−0.015 (0.885)	−0.121 (0.256)	−0.025 (0.818)	−0.143 (0.179)	1	0.302 ** (0.004)	0.251 * (0.017)	0.374 ** (0)	0.226 * (0.032)	0.347 ** (0.001)
The number of residents	0.273 ** (0.009)	−0.309 ** (0.003)	0.246 * (0.019)	−0.109 (0.304)	0.302 ** (0.004)	1	0.865 ** (0)	0.819 ** (0)	0.875 ** (0)	0.892 ** (0)
Public service convenience	0.466 ** (0)	−0.317 ** (0.002)	0.435 ** (0)	0.012 (0.914)	0.251 * (0.017)	0.865 ** (0)	1	0.762 ** (0)	0.817 ** (0)	0.919 ** (0)
Employment opportunities	0.174 (0.102)	−0.119 (0.263)	0.143 (0.18)	−0.163 (0.125)	0.374 ** (0)	0.819 ** (0)	0.762 ** (0)	1	0.890 ** (0)	0.866 ** (0)
The richness of cultural and Recreational facilities	0.211 * (0.046)	−0.216 * (0.041)	0.184 (0.082)	−0.178 (0.094)	0.226 * (0.032)	0.875 ** (0)	0.817 ** (0)	0.890 ** (0)	1	0.889 ** (0)
Transportation convenience	0.397 ** (0)	−0.279 ** (0.008)	0.355 ** (0.001)	−0.081 (0.448)	0.347 ** (0.001)	0.892 ** (0)	0.919 ** (0)	0.866 ** (0)	0.889 ** (0)	1

Note: ** and * indicate 1% and 5% significance levels, respectively.

In summary, aggregated green infrastructures with a carbon sequestration range of 0.1922–7.5511 t/a and location entropy range of 0.0387–1 were mainly distributed in the areas of the old urban area. These aggregated green infrastructures are the most attractive to socioeconomic activities.

4. Discussion

4.1. Carbon Sink Performance of Urban Aggregated Green Infrastructure

According to the latest urban planning of Nanjing, the urban green infrastructure construction focuses on the northwest and southwest regions. These regions overlap with most of the green infrastructure concentration areas with low carbon sink performance in our results. It is noteworthy that the carbon sink performance of the concentrated green infrastructure in the urban centre area does not perform well in our study findings. However, this part of the region has not received much attention from policy makers. Kopecka, M. et al. study of urban aggregated green infrastructure in Slovakia showed the limitations of Sentinel-2A data in identifying tree and shrub cover. This is similar to our identification results. Therefore, we used the average of the carbon sink coefficients of trees and shrubs from previous studies as the carbon sink coefficients of woodlands. We more accurately calculated the carbon sink performance of tree and shrub covered land for urban aggregated green infrastructure compared to the study of Kopecka, M. et al. [32].

There have been studies on urban green carbon sinks, mainly involving macro-level studies on large-scale urban forests and fine-scale studies on the carbon sink capacity of individual vegetation type [26,49]. The results on the carbon sink performance of aggregated green infrastructure at the city level are scarce due to data precision limitations. As the resolution of the Sentinel-2A satellite is high enough, we try to use it to discern aggregated green infrastructure within cities. In addition, we analysed the spatial distribution characteristics in areas with concentrated urban functions through spatial autocorrelation. It has been shown that spatial autocorrelation can analyse the correlation of the same variable in different spatial locations and is a measure of the degree of agglomeration in a spatial domain. At present, it is mostly applied to studies where the economic geography has obvious polarization and diffusion effects or the ecological environment has obvious regional differentiation characteristics [50,51]. In this paper, global spatial autocorrelation and local spatial autocorrelation are introduced to identify the spatial agglomeration characteristics of carbon sink performance of aggregated green infrastructure in metropolitan areas. Our results show that the aggregated green infrastructure with excellent carbon sink performance exhibits aggregation effect spatially. The clusters with poor carbon sink performance are relatively dispersed. In the future, we should focus on the concentrated areas of aggregated green infrastructures with poor carbon sink performance. Based on previous studies and the findings of this study, we conclude that concentrating the clus-

tered green infrastructure with excellent carbon sink performance can bring about better carbon sink effects [34,52–54]. Therefore, we suggest focusing on optimizing the existing clustered green infrastructure with poor carbon sink performance. The best carbon sink performance of the forest floor in this study. In addition, some studies have indicated that tree species with large leaf area have better carbon sink capacity due to their excellent photosynthetic effect [55,56]. In summary, we could reasonably increase the proportion of tree species with larger leaf area for optimizing the carbon sink performance of aggregated green infrastructure. It is advisable to build small aggregated green infrastructure with excellent carbon sink performance in areas where aggregated green infrastructure with poor carbon sink performance is concentrated to produce better carbon sink effects.

4.2. Effects of Human Socioeconomic Activities

Due to previous urban development and pristine topography, socioeconomic activities are concentrated in the urban centre and the southwest part of the city. In particular, those aggregated green infrastructures with excellent vegetation conditions and potentially better carbon sink performance are concentrated in the northeastern part of the city. These areas are not densely populated with socioeconomic activities and have a higher topography. This is generally consistent with the results of our study. Dietmar Sattler et al. showed that topographic conditions are an important influence on the performance of vegetation carbon sinks in Brazil. The carbon sink performance of vegetation with flat topography was better than that of sloping land [57]. This has some differences with our study. We consider that it is mainly related to the dense population around urban aggregated green infrastructure in China, which is more influenced by socioeconomic activities.

Many studies found that carbon sink changes are closely related to human activities. Zhang's study shows that aggregated green infrastructure carbon sinks are significantly influenced by human activities [58]. The more intensive the human activity, the worse the carbon sink capacity. Previously, human activity data have been studied using nighttime lights, population-kilometre grid, official government data, etc. [59–61]. Since the data are macro-level, it is difficult to reflect the socioeconomic situation within urban cities. POI data are immediate and flexible. As a result, they are excellent for research exploring socio-economic activities inside and outside the city. In this study, we introduce six types of POI data representing socioeconomic activities to analyse their correlation with aggregated green infrastructure carbon sink performance [14]. The results showed that aggregated green infrastructure with carbon sink (0.1922–7.5511 t/a) and locational entropy (0.0387-1) had the strongest effect on the aggregation of socioeconomic activities. Most of these clustered green infrastructures have an area of less than 25 ha and a spacing of less than 0.3. This represents a concentration of socioeconomic activities in the surrounding area, although the carbon sink performance of small and medium-sized strip aggregated green infrastructures is poor. Obviously, it is difficult to add large and medium-sized aggregated green infrastructure in densely populated and resource-intensive urban centres. We can build small aggregated green infrastructures in appropriate spaces. This will greatly improve the performance of the urban ecosystem carbon sink. It is advisable to build ecological corridors along the strip-shaped spaces such as roads and river. Although the carbon sink performance of ribbon aggregated green infrastructure is poorer than that of compact aggregated green infrastructure, the results of this study and some previous findings suggest that the aggregation effect of ribbon green infrastructure on socioeconomic activities is stronger. In general, the establishment of ecological corridors along ribbon spaces such as roads and rivers are desirable. This is a way to strengthen the links between different green infrastructures. It is preferable to plant trees with larger leaves and increase species richness to enhance carbon sink capacity [62–64].

4.3. Research Limitations and Future Development Direction

The present study has two main limitations. One limitation is that we used coefficients from previous studies for the carbon sink calculations, which may be different from the

actual situation. Another limitation is that the POI data lack comparisons of socioeconomic activities in the same region over time. It is weaker than traditional data in responding to a period of time. Combining previous studies and the findings of this study, we suggest the following future directions: (1) Sentinel-2A is a new satellite with high accuracy that performs well for the measurement of green infrastructure carbon sinks within cities. It could be used as a new way for fine-scale carbon sink research. (2) POI is a flexible and instantaneous data representing urban socioeconomic activities. It could be widely applied to the study of human–ecosystem interaction in the future. (3) Spatial autocorrelation is a method to study the spatial aggregation relationship of geographical elements. It could be used as an interdisciplinary research method in ecology in the future to study the spatial relationship of ecological elements within cities.

5. Conclusions

This study was conducted based on the Sentinel-2A satellite, combining it with six types of socioeconomic activities POI. We calculated the carbon sink performance of 90 aggregated green infrastructures. In addition, the carbon sequestration and location entropy spatial aggregation relationships of 79 street aggregated green infrastructures were evaluated by spatial autocorrelation methods. The results showed that the carbon sequestration and location entropy of aggregated green infrastructures in the northeastern part of the city were higher than those in the southwestern part. However, socioeconomic activities are more dispersed in the northeastern part, while they were more intensive in the southwest. This indicated a spatial distribution inconsistency between Socioeconomic activities and carbon sink performance in aggregated green infrastructures. Due to the dense urban development caused by resource constraints and topographic constraints, the aggregated green infrastructures area was different, and the connection was insufficient, resulting in the differentiation of Socioeconomic activities needs. Overall, our study provides to a new direction for calculating the carbon sink performance of urban aggregated green infrastructure at a fine scale. Moreover, we also reveal in depth the pattern between the carbon sink performance of urban aggregated green infrastructure and human socioeconomic activities. It is critical for more efficient utilization of carbon sink performance of urban aggregated green infrastructure in the future. The most important point is that these findings provide an important reference for green infrastructure planning in urban areas with intensive human socioeconomic activities. They indicate the way to achieve carbon neutrality in cities.

Author Contributions: Conceptualization, S.C. and Y.C.; methodology, S.C.; software, S.C.; validation, S.C., Y.C. and X.H.; formal analysis, S.C.; investigation, S.C.; resources, S.C.; data curation, H.D.; writing—original draft preparation, S.C.; writing—review and editing, S.C.; visualization, X.H.; supervision, J.L.; project administration, Y.C.; funding acquisition, Y.C. All authors have read and agreed to the published version of the manuscript.

Funding: This research was funded by Jiangsu Provincial Agricultural Science & Technology Independent Innovation Fund Project (No. CX (21) 3178).

Institutional Review Board Statement: Not applicable.

Informed Consent Statement: Not applicable.

Data Availability Statement: Not applicable.

Conflicts of Interest: The authors declare no conflict of interest.

References

1. Angel, S.; Parent, J.; Civco, D.L.; Blei, A.; Potere, D. The dimensions of global urban expansion: Estimates and projections for all countries, 2000–2050. *Prog. Plan.* **2011**, *75*, 53–107. [CrossRef]
2. Gaede, J.; Meadowcroft, J. A Question of Authenticity: Status Quo Bias and the International Energy Agency's World Energy Outlook. *J. Environ. Pol. Plan.* **2016**, *18*, 608–627. [CrossRef]
3. Zhang, M.; Wang, W.W. Analysis of spatial distribution of global energy-related CO_2 emissions. *Nat. Hazards* **2014**, *73*, 165–171. [CrossRef]

4. Shi, X.L.; Wang, T.L.; Lu, S.Y.; Chen, K.; He, D.; Xu, Z. Evaluation of China's forest carbon sink service value. *Environ. Sci. Pollut. Res.* **2022**, *29*, 44668–44677. [CrossRef] [PubMed]
5. Eze, S.; Palmer, S.M.; Chapman, P.J. Response to comments by Hoffmann et al. on "Upland grasslands in Northern England were atmospheric carbon sinks regardless of management regime". *Agric. For. Meteorol.* **2019**, *264*, 366–368. [CrossRef]
6. Bu, X.Y.; Dong, S.C.; Mi, W.B.; Li, F.J. Spatial-temporal change of carbon storage and sink of wetland ecosystem in arid regions, Ningxia Plain. *Atmos. Environ.* **2019**, *204*, 89–101.
7. Liu, C.; Liu, G.Y.; Casazza, M.; Yan, N.Y.; Xu, L.Y.; Hao, Y.; Franzese, P.P.; Yang, Z.F. Current Status and Potential Assessment of China? Ocean Carbon Sinks. *Environ. Sci. Technol.* **2022**, *56*, 6584–6595. [CrossRef]
8. Barthel, S.; Parker, J.; Ernstson, H. Food and green space in cities: A resilience Lens on gardens and urban environmental movements. *Urban Stud.* **2015**, *52*, 1321–1338. [CrossRef]
9. Biernacka, M.; Kronenberg, J. Classification of institutional barriers affecting the availability, accessibility and attractiveness of urban green spaces. *Urban For. Urban Green.* **2018**, *36*, 22–33. [CrossRef]
10. Ying, J.; Zhang, X.J.; Zhang, Y.Q.; Bilan, S. Green infrastructure: Systematic literature review. *Ekon. Istraz.* **2022**, *35*, 343–366. [CrossRef]
11. Wei, J.X.; Li, H.B.; Wang, Y.C.; Xu, X.Z. The Cooling and Humidifying Effects and the Thresholds of Plant Community Structure Parameters in Urban Aggregated Green Infrastructure. *Forests* **2021**, *12*, 111. [CrossRef]
12. Richard, T.F. Some general principles of landscape and regional ecology. *Landsc. Ecol.* **1995**, *10*, 133–142.
13. Iversen, M.H.; Lampitt, R.S. Size does not matter after all: No evidence for a size-sinking relationship for marine snow. *Prog. Oceanogr.* **2020**, *189*, 102445. [CrossRef]
14. Fan, P.; Xu, L.; Yue, W.; Chen, J. Accessibility of public urban green space in an urban periphery: The case of Shanghai. *Landsc. Urban Plan.* **2017**, *165*, 177–192. [CrossRef]
15. Kuwae, T.; Crooks, S. Linking climate change mitigation and adaptation through coastal green-gray infrastructure: A perspective. *Coast Eng. J.* **2021**, *63*, 188–199. [CrossRef]
16. McConnell, K.; Braneon, C.V.; Glenn, E.; Stamler, N.; Mallen, E.; Johnson, D.P.; Pandya, R.; Abramowitz, J.; Fernandez, G.; Rosenzweig, C. A quasi-experimental approach for evaluating the heat mitigation effects of roofs in Illinois. *Sust. Cities Soc.* **2022**, *76*, 103376. [CrossRef]
17. Zhu, S.J.; Yang, Y.; Yan, Y.; Causone, F.; Jin, X.; Zhou, X.; Shi, X. An evidence-based framework for designing urban green infrastructure morphology to reduce urban building energy use in a hot-humid climate. *Build. Environ.* **2022**, *219*, 109181. [CrossRef]
18. Chen, W.Y. The role of urban green infrastructure in offsetting carbon emissions in 35 major Chinese cities: A nationwide estimate. *Cities* **2015**, *44*, 112–120. [CrossRef]
19. Hsu, K.W.; Chao, J.C. Study on the Value Model of Urban Green Infrastructure Development-A Case Study of the Central District of Taichung City. *Sustainability* **2021**, *13*, 7402. [CrossRef]
20. Jantz, C.A.; Manuel, J.J. Estimating impacts of population growth and land use policy on ecosystem services: A community-level case study in Virginia, USA. *Ecosyst. Serv.* **2013**, *5*, 110–123. [CrossRef]
21. Huang, C.D.; Shao, Y.; Liu, J.H.; Chen, J.S. Temporal analysis of urban forest in Beijing using Landsat imagery. *J. Appl. Remote Sens.* **2007**, *1*, 013534. [CrossRef]
22. Westfall, J.A. A Comparison of Above-Ground Dry-Biomass Estimators for Trees in the Northeastern United States. *North. J. Appl. For.* **2012**, *29*, 26–34. [CrossRef]
23. Snehlata; Rajlaxmi, A.; Kumar, M. Urban tree carbon density and CO_2 equivalent of National Zoological Park, Delhi. *Environ. Monit. Assess.* **2021**, *193*, 841. [CrossRef] [PubMed]
24. Yin, G.F.; Zhao, N.J.; Shi, C.Y.; Chen, S.; Qin, Z.S.; Zhang, X.L.; Yan, R.F.; Gan, T.T.; Liu, J.G.; Liu, W.Q. Phytoplankton photosynthetic rate measurement using tunable pulsed light induced fluorescence kinetics. *Opt. Express.* **2018**, *26*, 293–300. [CrossRef]
25. Kinnunen, A.; Talvitie, I.; Ottelin, J.; Heinonen, J.; Junnila, S. Carbon sequestration and storage potential of urban residential environment-A review. Sust. *Cities Soc.* **2022**, *84*, 104027. [CrossRef]
26. Lahoti, S.; Lahoti, A.; Joshi, R.K.; Saito, O. Vegetation Structure, Species Composition, and Carbon Sink Potential of Urban Green Spaces in Nagpur City, India. *Land* **2020**, *9*, 107. [CrossRef]
27. Zhang, X.X.; Brandt, M.; Tong, X.W.; Ciais, P.; Yue, Y.M.; Xiao, X.M.; Zhang, W.M.; Wang, K.L.; Fensholt, R. A large but transient carbon sink from urbanization and rural depopulation in China. *Nat. Sustain.* **2022**, *5*, 321–328. [CrossRef]
28. Ma, X.P.; Li, J.; Zhao, K.F.; Wu, T.; Zhang, P.T. Simulation of Spatial Service Range and Value of Carbon Sink Based on Intelligent Urban Ecosystem Management System and Net Present Value Models-An Example from the Qinling Mountains. *Forests* **2022**, *13*, 407. [CrossRef]
29. Lorenzo-Saez, E.; Lerma-Arce, V.; Coll-Aliaga, E.; Oliver-Villanueva, J.V. Contribution of green urban areas to the achievement of SDGs. Case study in Valencia (Spain). *Ecol. Indic.* **2021**, *131*, 108246. [CrossRef]
30. Penazzi, S.; Accorsi, R.; Manzini, R. Planning low carbon urban-rural ecosystems: An integrated transport land-use model. *J. Clean Prod.* **2019**, *235*, 96–111. [CrossRef]
31. Xia, L.L.; Wei, J.F.; Wang, R.W.; Chen, L.; Zhang, Y.; Yang, Z.F. Exploring Potential Ways to Reduce the Carbon Emission Gap in an Urban Metabolic System: A Network Perspective. *Int. J. Environ. Res. Public Health* **2022**, *19*, 5793. [CrossRef] [PubMed]

32. Kopecka, M.; Szatmari, D.; Rosina, K. Analysis of Urban Green Spaces Based on Sentinel-2A: Case Studies from Slovakia. *Land* **2017**, *6*, 25. [CrossRef]
33. Wang, L.; Zhou, Y.; Liu, J.Y.; Liu, Y.J.; Zuo, Q.; Li, Q. Exploring the potential of multispectral satellite images for estimating the contents of cadmium and lead in cropland: The effect of the dimidiate pixel model and random forest. *J. Clean Prod.* **2022**, *367*, 132922. [CrossRef]
34. Silva, L.O.E.; Resende, M.; Galhardas, H.; Manquinho, V.; Lynce, I. DeepData: Machine learning in the marine ecosystems. *Expert Syst. Appl.* **2022**, *206*, 117841. [CrossRef]
35. Tripp, H.L.; Crosman, E.T.; Johnson, J.B.; Rogers, W.J.; Howell, N.L. The Feasibility of Monitoring Great Plains Playa Inundation with the Sentinel 2A/B Satellites for Ecological and Hydrological Applications. *Water* **2022**, *14*, 2314. [CrossRef]
36. Biswas, R.; Rathore, V.S.; Krishna, A.P.; Singh, G.; Das, A.K. Integration of C-band SAR and high-resolution optical images for delineating palaeo-channels in Nagaur and Barmer districts, western Rajasthan, India. *Environ. Monit. Assess.* **2022**, *194*, 589. [CrossRef]
37. Yu, D.J.; Wanyan, W.B.; Wang, D.J. Leveraging contextual influence and user preferences for point-of-interest recommendation. *Multimed. Tools Appl.* **2021**, *80*, 1487–1501. [CrossRef]
38. Liu, K.; Yin, L.; Lu, F.; Mou, N.X. Visualizing and exploring POI configurations of urban regions on POI-type semantic space. *Cities* **2020**, *99*, 102610. [CrossRef]
39. Bin, C.Z.; Gu, T.L.; Sun, Y.P.; Chang, L. A personalized POI route recommendation system based on heterogeneous tourism data and sequential pattern mining. *Multimed. Tools Appl.* **2019**, *78*, 35135–35156. [CrossRef]
40. Rahmani, H.A.; Deldjoo, Y.; di Noia, T. The role of context fusion on accuracy, beyond-accuracy, and fairness of point-of-interest recommendation systems. *Expert Syst. Appl.* **2022**, *205*, 117700. [CrossRef]
41. Zhao, S.J.; Duan, W.C.; Zhao, D.F.; Song, Q.B. Identifying the influence factors of residents? low-carbon behavior under the background of "Carbon Neutrality": An empirical study of Qingdao city, China. *Energy Rep.* **2022**, *8*, 6876–6886. [CrossRef]
42. Zhang, X.X.; Lu, Z.G.; He, M.G.; Wang, J.F. What can Beijing learn from the world megacities on energy and environmental issues? *Energy Rep.* **2022**, *8*, 414–424. [CrossRef]
43. Zhang, Y.; Wang, Q.; Li, B. Study on forecasting ecological land demand with carbon-oxygen balance method. *China Lands Cience* **2008**, *6*, 23–28. (In Chinese)
44. Jie, H.; Pan, Y.; Zhu, W. Measurement of terrestrial ecosystem service value in China. *Chin. J. Ecol.* **2005**, *6*, 1122–1127. (In Chinese)
45. Xueying, M.; Xiufeng, Z. Carbon storage and fixation by a typical wetland vegetation in Changjiang River Estuary—A case study of Phragmites australis in east beach of Chong Ming Island. *Chin. J. Eco-Agric.* **2008**, *2*, 269–272. (In Chinese)
46. Xiaonan, D.; Xiaoke, W.; Fei, L. Carbon sequestration and its potential by wetland ecosystems in China. *J. Ecol.* **2008**, *2*, 463–469. (In Chinese)
47. Cao, Z.Y.; Yan, Y.C.; Tang, K. Path optimization of open collaborative innovation of energy industry in urban agglomeration based on particle swarm optimization algorithm. *Energy Rep.* **2022**, *8*, 5533–5540. [CrossRef]
48. Gu, Y.X.; Li, W.; He, G.; Zhao, S.H. Evaluation of industrial ecological security in industrial transformation demonstration area based on spatiotemporal differentiation. *Geomat. Nat. Hazards Risk* **2022**, *13*, 1422–1440.
49. Ariluoma, M.; Ottelin, J.; Hautamaki, R.; Tuhkanen, E.M.; Manttari, M. Carbon sequestration and storage potential of urban green in residential yards: A case study from Helsinki. *Urban For. Urban Green.* **2021**, *57*, 126939. [CrossRef]
50. Park, Y.; Kim, S.H.; Kim, S.P.; Ryu, J.; Yi, J.; Kim, J.Y.; Yoon, H.J. Spatial autocorrelation may bias the risk estimation: An application of eigenvector spatial filtering on the risk of air pollutant on asthma. *Sci. Total Environ.* **2022**, *843*, 157053. [CrossRef]
51. Zhang, X.Y.; Zhang, R.; Zhao, M.L.; Wang, Y.; Chen, X. Policy Orientation, Technological Innovation and Energy-Carbon Performance: An Empirical Study Based on China's New Energy Demonstration Cities. *Front. Environ. Sci.* **2022**, *10*, 846742. [CrossRef]
52. Mahanta, N.K.; Abramson, A.R. The thermal flash technique: The inconsequential effect of contact resistance and the characterization of carbon nanotube clusters. *Rev. Sci. Instrum.* **2012**, *83*, 054904. [CrossRef]
53. Wu, Q.; Lin, Q.G.; Yang, Q.; Li, Y. An optimization-based CCUS source-sink matching model for dynamic planning of CCUS clusters. *Greenh. Gases* **2022**, *12*, 433–453. [CrossRef]
54. Guo, H.Q.; Yu, Q.; Pei, Y.R.; Wang, G.; Yue, D.P. Optimization of landscape spatial structure aiming at achieving carbon neutrality in desert and mining areas. *J. Clean Prod.* **2021**, *322*, 129156. [CrossRef]
55. Mickler, R.A.; Fox, S. Effects of elevated carbon dioxide on the growth and physiology of loblolly pine. In *The Productivity and Sustainability of Southern Forest Ecosystems in a Changing Environment*; Springer: New York, NY, USA, 1998; Volume 128, pp. 93–101.
56. Lopez, M.L.; Gerasimov, E.; Machimura, T.; Takakai, F.; Iwahana, G.; Fedorov, A.N.; Fukuda, M. Comparison of carbon and water vapor exchange of forest and grassland in permafrost regions, Central Yakutia, Russia. *Agric. For. Meteorol.* **2008**, *148*, 1968–1977. [CrossRef]
57. Sattler, D.; Murray, L.T.; Kirchner, A.; Lindner, A. Influence of soil and topography on aboveground biomass accumulation and carbon stocks of afforested pastures in South East Brazil. *Ecol. Eng.* **2014**, *73*, 126–131. [CrossRef]
58. Chen, Y.G. An analytical process of spatial autocorrelation functions based on Moran's index. *PLoS ONE* **2021**, *16*, e0249589. [CrossRef]
59. Meng, X.; Han, J.; Huang, C. An Improved Vegetation Adjusted Nighttime Light Urban Index and Its Application in Quantifying Spatiotemporal Dynamics of Carbon Emissions in China. *Remote Sens.* **2017**, *9*, 829. [CrossRef]

60. Rizzati, M.; De Cian, E.; Guastella, G.; Mistry, M.N.; Pareglio, S. Residential electricity demand projections for Italy: A spatial downscaling approach. *Energy Policy* **2022**, *160*, 112639. [CrossRef]
61. Zhang, H.; Bi, Y.; Kang, F.; Wang, Z. Incentive mechanisms for government officials' implementing open government data in China. *Online Inf. Rev.* **2022**, *46*, 224–243. [CrossRef]
62. Steffens, C.; Beer, C.; Schelfhout, S.; De Schrijver, A.; Pfeiffer, E.M.; Vesterdal, L. Do tree species affect decadal changes in soil organic carbon and total nitrogen stocks in Danish common garden experiments? *Eur. J. Soil Sci.* **2021**, *73*, 13206. [CrossRef]
63. Beckert, M.R.; Smith, P.; Lilly, A.; Chapman, S.J. Soil and tree biomass carbon sequestration potential of silvopastoral and woodland-pasture systems in North East Scotland. *Agrofor. Syst.* **2016**, *90*, 371–383. [CrossRef]
64. Hulvey, K.B.; Hobbs, R.J.; Standish, R.J.; Lindenmayer, D.B.; Lach, L.; Perring, M.P. Benefits of tree mixes in carbon plantings. *Nat. Clim. Chang.* **2013**, *3*, 869–874. [CrossRef]